AD NUMBER

AD307953

CLASSIFICATION CHANGES

TO: unclassified

FROM: secret

LIMITATION CHANGES

TO:

Approved for public release, distribution unlimited

FROM:

Distribution authorized to DoD only; Administrative/Operational use; 1 Sep 1957. Other requests shall be referred to Diamond Ordnance Fuze Labs, Attn: Technical Information Branch, Washington, DC 20310.

AUTHORITY

d/a ltr, 15 Aug 1979; d/a ltr, 15 Aug 1979

SECRET

REGRADING DATA CANNOT BE PREDETERMINED

A SENSING SYSTEM FOR DASH-DOT (U)

TA3-9108
DA506-01-011

1 September 1959

TR-470
65 Pages
Copy No. 26

By

L. Melamed H. W. Straub

H. R. Ulrich

FOR THE COMMANDER:

Approved by

H. P. Kalmus
Chief, Laboratory 50

DIAMOND ORDNANCE FUZE LABORATORIES
ORDNANCE CORPS • • • DEPARTMENT OF THE ARMY

SECRET

DIAMOND ORDNANCE FUZE LABORATORIES
ORDNANCE CORPS WASHINGTON 25, D. C.

A SENSING SYSTEM

FOR DASH-DOT (U)

TA3-9108 1 September 1957 TR-470
DA506-01-011 65 Pages
DOFL Proj. 52850 Copy No.___

By

L. Melamed H. W. Straub

R. R. Ulrich

FOR THE COMMANDER:

Approved by

for
H. P. Kalmus
Chief, Laboratory 50

SECRET

CONTENTS

ABSTRACT (S)

A system of dynamic armor for tanks (Dash-Dot) is under investigation. A successful system will sense the presence of an anti-tank round, compute its trajectory, and defeat it by automatically firing defending charges that will destroy the attacking rounds before impact. A sensing system of three optical screens, employing filtered IR sources and photoconductive detectors (PbS cells) has been devised. Preliminary evaluations of the physical and geometrical detection parameters are discussed. In tests of an experimental screen system, an accuracy of about 2% has been achieved in determining the unknown altitude and velocity of 75 mm shells at velocities up to 2500 fps. Preliminary calculations on the complete geometry of the system are presented as an appendix.

I. INTRODUCTION

A system of dynamic armor for tanks (Dash-Dot) is under investigation. A successful system will sense the presence of an anti-tank round, compute its trajectory, and defeat it by automatically firing defending charges that will destroy the attacking rounds before impact.

Protection is desired from attacking rounds in the velocity range of from 200 fps to a maximum of 5000 fps. The system should be operative day and night under a wide variety of climatic and terrain conditions.

Three major problem areas to be considered are:

1. Physical detection
2. Geometry of the detection screen
3. Computation

This paper is concerned with only the first two general problems, treated together.

II. SYSTEM REQUIREMENTS

Broadly, the system requirements are:

1. To determine missile trajectory in a "sufficiently short" time.
2. To ignore objects with velocities less than 200 fps.

3. To ignore small arms fire.

4. To be insensitive to ambient conditions of sun and sky light.

5. To fire defending charges whose fragment velocity must be several times that of the fastest attacking round.

A feasibility study was undertaken using energy in the optical spectrum. One obvious advantage here is the high spatial resolution available which makes possible accurate position and velocity determination. A 3-layer optical sensing screen was conceived to surround the tank as shown in figure 1. The defending linear charges form the fourth innermost layer. Each sensing layer consists of a series of uniformly spaced IR sources and detectors mounted in reflection optics: b_0, b_1, b_2 represent the three detection cone axes; P_c represents the direction of flight of the defending charge. It is assumed that the attacking rounds move in or nearly in the horizontal plane and will intersect at least one detection cone in each of the three layers. Axes b_0 and b_1 are parallel to each other; axes b_1 and b_2 are at some fixed angle. The direction of P_c lies between the vertical and the "b_2" direction.

For normal incidence, the transit times between the three layers yield the velocity and altitude directly. For other than normal incidence (general case) the transit times will be functions of the amount of obliquity and the effective separations x and y will be increased proportionally. This amount of obliquity (angle of approach) is determined after the missile has penetrated the first two layers and will determine which charge or charges of the array need be fired. The 3-layer sensing screen is effectively a 3-dimensional switchboard with contacts being made optically. Appendix A derives the basic equations that the computer will be required to handle.

III. DETECTION PHILOSOPHY

1. Source Modulation

The possibility of amplitude modulation of the emitted energy was investigated. This approach did not prove fruitful for the present system due to a lack of suitable source-detector combination modulatable at the required frequencies. If recognition were required within six inches after a 4000 fps missile penetrated a beam, an 80 kc source would yield about 10 pulses.

$$\text{i.e., available time} = \frac{\frac{1}{2}}{4000} \text{ seconds} = \frac{1}{8} \text{ ms}$$

Ultra-violet sources are available which may be efficiently modulated at this frequency but are too large for use in focusing optics. A tungsten filament bulb may be modulated up to about 25 kc but with very poor efficiency. Meagre success was achieved in attempting to modulate an ultra-small, glass enclosed zirconium arc; at 1000 cps the modulation had dropped to 5%.

2. Steady "DC" Source

All work to date has utilized a steady light source furnishing a single reflected light pulse. To achieve high spatial resolution it is necessary to keep the source and especially the detector area as small as possible (relative to the reflector aperture). Although small-area phototubes (e.g. 1P42) are available, the most efficient source-detector combination has proven to be a tungsten-filament source and a photo-conductive detector. The source used is a 6-volt, 0.5 ampere PR-12 flashlight bulb having an effective radiating area of about 1 mm^2. When operated at its rated voltage, it has peak emission at about 1.29 μ. By lowering the applied voltage, the emission peak may be conveniently shifted to longer wavelengths matching available detectors. At 0.8 volts, for example, peak emission occurs at about 2.0μ.

IV. DETECTOR REQUIREMENTS

1. Basic Considerations

A fundamental requirement of a suitable detector is a short rise-time constant and an adequate S/N response for the fastest rounds at the greatest anticipated detection distance ("h" in figure 1).[1] Under some of the worst conditions of operation, pulses in successive channels might occur 100 μs apart. For adequate time resolution, it would be necessary to reach a decision in about 25 μs. The time constant, sensitivity, and noise of various IR detectors were investigated to determine the most promising detector presently available. The photo-conductive type of IR detector seemed attractive because of minute size, easy alteration of sensitive area, ruggedness, non-

[1] System is not drawn to any particular scale.

microphonism, high IR sensitivity, and simple power supply and circuitry demands. Among the cells tested for ambient temperature use were an E.C.A.[2] Pbs cell, an Ektron Pbs cell, and a typical S.B.R.C.[3] PbSe cell. All the cells were of the chemically deposited type. The E.C.A. cell had a 2.5 mm x 2.5 mm sensitive area; the other two were 1 mm x 1 mm in area. A "point" source of light was mechanically modulated; the output signal was fed to a low-noise amplifier and measured on an oscilloscope.

2. Time Constant Measurements

To measure time constants, a ninety-slot chopping wheel was constructed which could be rotated at any desired speed between 30 rpm and 22,000 rpm providing a "square" wave interruption frequency from about 45 cps to about 33 kc. The slot width was 2.2 mm. Thus, since the cell area exposed was 1 mm wide in all cases, the input was actually trapezoidal, neglecting diffraction effects.

3. Noise Measurements

The noise of a photo-conductive detector is generally taken to be the pure current noise, E_3, due to random fluctuations in the steady-state current. As is well known, such noise varies as $\frac{1}{f}$ where f = frequency.

The observed noise = E where

$$E = \sqrt{E_1^2 + E_2^2 + E_3^2} \text{ volts P.T.P}$$

E_1 = Amplifier noise referred to the input.

E_2 = Johnson noise developed across the cell and load.

E_3 = Current noise.

---

2 Electronics Corporation of America

3 Santa Barbara Research Center

As the bias voltage is increased both the signal and S/N increase to a maximum value and then decay. The optimum voltage occurs for a power dissipation of about $0.1 \frac{\text{watts}}{\text{cm}^2}$ on the detector.[1] This figure has been roughly confirmed for the present cells. Utilizing the 25 μs maximum decision time previously mentioned, one can compute what the minimum chopping frequency should be at which S/N of various detectors should be compared. Thus a long time-constant detector with excellent sensitivity may yield a superior S/N at high frequencies than will a short time-constant detector with mediocre sensitivity. This has proven to be the case. From the geometry of the chopper, the cell is illuminated fro 25 μs at the frequency of about 14,000 cps. Figure 2 lists the normalized responses of the 3 cells as a function of chopping frequency. Time did not permit testing more than 1 sample of each type.

A bare tungsten lamp peaked at 1.3 μ supplied a field intensity of 205 $\frac{\mu \text{ w}}{\text{cm}^2}$ for each cell.[2] At 14,000 cps the Ektron cell yielded the largest S/N ratio. In comparing the S/N ratio , a small correction should be made for the different spectral sensitivities of room temperature PbS and PbSe. The "half-power" spectral response points of a typical 25°C PbS cell are at $\sim$1μ and $\sim$2.8μ; for a typical 25°C PbSe cell (S.B.R.C.) they occur at $\sim$1μ and $\sim$4.5μ (see figure 3). For a theoretical black body peaked at 1.3μ, 16% of the energy emitted lies between 2.8μ and 4.5μ. An additional correction should be made for the larger mismatch between the PbSe cell ($\sim$3.5μ peak) and the source (1.3μ) as compared to the PbS ($\sim$2.0μ peak) cell and the same source. Because of the non-symmetry of the black body emission curve and of the typical photo-conductor curve about their respective peaks, optimum response should occur for a radiator whose peak occurs at a shorter wavelength than that of the detector. The optimum amount of mismatch will be determined in future work.

Cell Area Effects

In a photoconductor,

$$N \propto \frac{1}{\sqrt{A}} \qquad (3)$$

N = current noise at a fixed bias
A = cell area

1 Verbally transmitted from R.M. Talley, NOL, White Oak, Maryland

2 Total emission to 9μ.

3 "Kodak Ektron Detector" handbook, page 7.

For a cell prefocussed in a given paraboloid, the energy incident on the cell is obviously independent of area. Thus, the S/N will improve as the cell area increases. However, the antenna pattern broadens as the sensitive area increases, lessening both the on-axis sensitivity and the directivity (resolution).

V. SENSING SCREEN

To establish feasibility it is first necessary to determine the expected signal level (single pulses) for a wide variety of operational parameters including missile size, shape of missile ogive, velocity, missile reflectivity, terrain reflectivity, ambient illumination, altitude, sensing angle, and circuit parameters. It is further necessary to determine the trajectory resolution. For these investigations, two sensing sub-screens were constructed. One of these is a 3-element single row sub-screen (figure 4); the other is a 9-element triple row sub-screen (figure 5)equipped with circuitry to display the angle of incidence visually by automatically switching on the appropriate neon bulbs on a display board after round passage. Each element consists of a source and detector, with axes parallel and in close proximity. The source is a PR-12 flashlight bulb operated at 5.00 volts and consuming 2.25 watts; the detector is a Kodak Ektron 1mm x 1 mm Pbs cell. Each is mounted at the focus of a small commercial parabolic reflector of about $1\frac{3}{4}$" diameter. The optical gain is about 400 for the source and about 200 for the detector; suitable shielding is employed to eliminate stray radiation. The radiation pattern for a 1 mm^2 source (or detector) in the reflector used is shown in figure 6. The "half-power" beam width is 3° included angle. Infrared transmission filters are available for operational security. These filters (figure 7) transmit about 90% in the 2μ region. The basic detector circuit is:

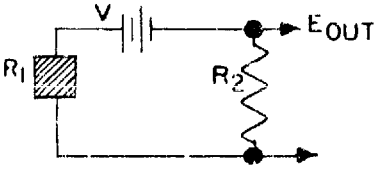

R_1 = Pbs cell

R_2 = Load resistor

R_2 was chosen equal to the dark resistance of the cell, approximately 800,000 ohms.

VI. MISSILE SIMULATORS

Various missile simulators have been conceived and constructed to investigate the response of the sub-screens. These have included laboratory air guns capable of propelling wood slugs(3" long, 3/4" diameter) at speeds up to 300 fps. The DOFL air gun facilities have been used to investigate detection parameters of Styrofoam rounds(12" long, 4" diameter) propelled at speeds up to 1000 fps. Tests are currently in progress at the DOFL Tes Area using inert 75 mm. rounds fired at speeds up to 2600 fps.

Figure 5 shows the laboratory setup utilizing the 9-element sub-screen with a small air gun. Figure 4 shows the experimental arrangement used in the DOFL air gun building using the 3-element sub-screen. Figure 8 illustrates the instrumentation room just outside the firing room. Shown are the gun control panel, the oscilloscope with a polaroid Land camera for recording target signals, electronic switches used to record the three separate pulses on a single photo and a counter used for independent checks on the optically recorded round velocity.

VII. GENERAL DETECTION PROBLEMS

As indicated previously, (p. 10) the pulse rise time and amplitude of the detector response will depend on many independent parameters of detection. In addition, both negative and positive pulses may be obtained depending on the relative reflectivities of target and background and upon the detection altitude. A negative signal is due to obscuration. Preliminary data on the contribution of each operational parameter will be given and an attempt will be made to tentatively evaluate their composite effect. Trajectory resolution measurements will then be described.

1. Signal vs Range

For detection distances large relative to the reflector aperture, simple theory predicts h^{-4} fall-off of signal with range for an active system. The observed variation of signal with distance does not fall off this rapidly due to (a) the aperture of the detector being not sufficiently large relative to the detection range, (b) the narrowness of the detection pattern beam and (c) the projected area of the target.

Point (a) requires no further comment. For rather narrow beams it is readily appreciated that at close-in distances only part of the missile is illuminated. At greater ranges, more of the target lies in the detection beam. If the ellipse formed by the detection cone and the plane in which the missile lies is completely enclosed by the projected area of the round, increasing the distance should produce no signal change since the flux density at the target would decrease as h^{-2} while the illuminated area would increase as h^{+2}. At such a distance that the ellipse minor axis equalled the missile diameter, the signal would start to fall off as h^{-1} until such an altitude is reached that the entire projected missile area lies within the detection ellipse. Beyond this range the signal should fall off as h^{-2}. For an illumination cone similar to and nearly co-axial with the detection cone the same argument holds. Thus at sufficiently high altitudes where h^{-2} fall-off holds, the net signal varies as $(h^{-2})(h^{-2}) = h^{-4}$ neglecting other limiting arguments. Since the beam pattern of the detector has no sharp limits but falls off gradually with increasing off-axis angle, a complete computation of signal return as afunction of range and missile size would be very difficult. Further, it will not always be true that the effective target area equals the projected target area. This holds strictly only for a Lambertian reflector.

In addition to these considerations, it is found for small objects that as the altitude is increased the return signal decreases smoothly through zero into negative going pulses. A zero signal return occurs at that altitude where the round obscures as much background-reflected energy as is directly reflected by the round. Experimental determinations of the effect of the detection altitude on signal have not been completed except for small objects(wooden pellets) expelled from a laboratory air gun and some partial data on Styrofoam rounds(figure 9).

2. Signal vs. Velocity

As missile velocities increase, the pulse height, rise time, and the pulse width decrease. The solid line of figure 9 shows the variation of pulse amplitude with velocity for 12" long Styrofoam rounds fired at speeds between 200 and 1000 fps. This plot is simply explained in terms of the average time constant of a cell. In addition, since the average time constant is known, the results may be readily extrapolated to higher velocities. The dotted portion shows the extrapolation to 5000 fps. The leveling-off of the "2.5 foot altitude" curve at speeds below about 400 fps

may be explained by taking into account the missile length, detection cone cross-section, and the time constant.

Thus, at 2.5 feet, the detection pattern (one cross-section for normal incidence is a circle of about 3.3" diameter. Since the rounds are 12" long, the time spent in the beam during which the radiation return is a maximum and stationary is,

$$t = \frac{\frac{12" - 3.3"}{12}}{v} \text{ seconds}$$

where v = velocity in fps.

If this time is equal to the rise time constant ($\sim$ 1.25 ms), we would expect the pulse amplitude to have reached 63.2% of its maximum value, i.e., $(1 - \frac{1}{e}) \times 100\%$. For t greater than the time constant, the peak amplitude should no longer increase with decreasing v. This is observed for the 2.5 foot altitude case. A simple computation confirms the correctness of this curve. Thus, at t = 1.25 ms,

$$v = \frac{\frac{12 - 3.3}{12}}{1.25 \times 10^{-3}} \text{ fps or } \sim 580 \text{ fps.}$$ From

figure 9, 63.2% of maximum occurs at v = $\sim$900 fps. The agreement is adequate since the time constants of the Ektron cells vary and since the total illumination time is actually

$$t_{total} = \frac{\frac{12 + 3.3}{12}}{v} \text{ seconds,}$$ counting time from the moment

the beam is just entered to when it is just cleared. On the latter basis, a time constant of 1.25 ms would yield a velocity

$$v = \frac{\frac{12 + 3.3}{12}}{1.25 \times 10^{-3}} \text{ fps} = 1{,}020 \text{ fps.}$$

Exact prediction is further complicated by the awkward geometrical problem of computing the rate of energy reflection generated when the target

ogive enters a "circular" detection region (of non-uniform sensitivity) at a constantly varying angle of incidence. The latter variation is due to ogive curvature. At an altitude of 5 feet, the detection cone cross-section is about 5" in diameter a' a smaller "time-constant velocity" should be expected. The data presented do not show a similar leveling off since velocities below 200. fps could not be conveniently obtained in the large air gun.

Rise times* have been measured for the velocity range 200 to 1000 fps at detection altitudes of 2.5 feet and 5 feet for Styrofoam rounds (normal incidence). The results are given in figure 10. Extrapolation to higher velocities is more difficult in this case than for the previous case (figure 9). Data is currently being taken at the DOFL Test Area that will show the relation between rise times and round velocities in the range of 1400-2600 fps for various altitudes utilizing 75 mm artillery shells and for angles of incidence of 30° and 45°.

In general, the rise time will depend in a complicated way on both the geometrical parameters and the detector time constants. For transit times greater than the cell time constant, only the geometrical factors (e.g. altitude, beam width, missile length, missile dia., etc.) are significant. For transit times less than the cell time constant, we should expect the peak amplitude as well as the rise time to decrease with increasing velocity. There is not sufficient data to show the predominating time-constant effect, except for the 2.5 foot curve in figure 9. From figure 10 it is apparent that a one-foot screen separation distance is adequate for the spatial resolution of rounds up to velocities of 1000 fps and altitudes of at least 5 feet. Thus, at an altitude of 2.5 feet and a speed of 300 fps, the observed rise time is 1.7 ms. This may be compared with the transit time between screens of

$$\frac{1 \text{ foot}}{300 \text{ fps}} \cong 3 \text{ ms.}$$

At an altitude of 5 feet the corresponding rise time is 2.8 ms. At 1000 fps, for both altitudes the rise time is approximately 1 ms; similarly, transit time is about 1 ms. For transit times shorter than 1 ms for a one-foot fence separation (i.e, for velocities greater than fps) the rate of decrease of rise time with decreasing transit time should diminish, requiring either that a greater fence separation be used or that recognition be accomplished in less than the rise time.

---

* The rise time shall be defined as the time it takes for the signal to go from 10% of peak to 90% of peak.

Thus

$\frac{d\tau}{dT^*}$ = constant up to about $T^* \approx 1$ ms

and $\frac{d\tau}{dT^*}$ decreases for $T^* < 1$ ms since detector time constant $\tilde{>}$ 1 ms

where

τ = rise time

T^* = transit time between 2 adjacent fences

Exact measurements of both the rate of rise of signal out of noise and of the relationship of missile ogive to the detection axis as the signal grows in time are being made for typical firings in the large air gun.

Microscopic examination of typical pulses (see figure 11a.) has yielded the provisional data (Table I).

The times referred to are for the signal to rise to the indicated level. These times are not uniquely related to the instantaneous position of the ogive relative to the detection cone.

5. Signal vs. Size

Pulse amplitudes of 4" diameter Styrofoam missiles of varying lengths were found to be approximately proportional to the missile length for detection altitudes of 2.5 feet and normal incidence. The round velocity was 800 fps for these tests. The rise time decreased with decreasing missile length. As before, assuming a beam diameter of about 3.3" at 2.5 feet altitude and a round velocity of 800 fps, it takes

$$\frac{3.3}{12} \text{ ft.} \Big/ 800 \text{ ft/sec.} = 0.34 \text{ ms}$$

for the round to achieve full illumination as it enters the beam. Since this time is less than the cell time constant ($\sim$ 1.2 ms), rounds longer than about 3.3" will increase the transit time through any one beam. In turn, leveling off will be produced near the top of the pulse, thereby increasing the rise time.

TABLE I. Pulse Data

Oscillogram	Velocity (fps)	Altitude (feet)	Signal (mv) 1st 200 μs	Signal (mv) 1st 400 μs	Noise* (mv)	S/N* (after 200 μs)	S/N* (after 400 μs)	Peak Signal (volts)	Time to peak (ms)
I	422	2.5	15	65	0.2	75	325	1.0	2.6
VII	650	2.5	30	100	"	150	500	0.8	1.6
V	960	2.5	50	170	"	250	850	0.64	1.1
4	310	5	2.5	4	"	12.5	20	0.38	4.2
7	640	5	4	10	"	20	50	0.22	2.0
9	970	5	7	30	"	35	150	0.14	1.1

*for a band pass of 10 → 150,000 cycles and a bias voltage = 45 volts.

TABLE II. Pulse Data

Oscillogram	Missile Length	Signal (mv) 1st 200 μs	Signal (mv) 1st 400 μs	Noise* (mv)	S/N* (after 200 μs)	S/N* (after 400 μs)	Peak Signal (volts)	Time to peak (ms)
1D	11"	29	100	0.2	145	500	.64	1.6
3D	5 1/2"	~15	~90	"	75	450	.36	1.1
4D	2 3/4"	~8	~60	"	30	300	.16	1

* for a band pass of 10 → 150,000 cycles and a bias voltage = 45 volts.

Table II presents these results (see figure 11B). In each case, the velocity is 800 fps, the altitude is 2.5 feet, and incidence is normal to the missile axis.

4. Target Reflectivity, Terrain reflectivity, and Sensing angle.

Relative reflecting powers of various substances in the entire 0.7 to 2.8 μ region of the spectrum have been measured. The reflectivity measured in each case is the relative return energy for a screen sub-element whose parallel axes are inclined at various sensing angles to either a flat simulated terrain, or to the line of flight of a simulated missile. These sensing angles range from normal incidence to 60° from normal.

To make these measurements, a reflectometer was designed and built. The sub-element is mounted on a rotating head whose center of curvature lies on the sample being measured. A Corning filter No. 7-56 was employed over the detector parabola. The source employed was a 6-volt PR-13 bulb operated at 1.20 volts. For normal incidence, the detection cone diameter at the test surface was about 3.3" in diameter. The results are given below in dimensionless form.

	Sensing Angle (off normal)					
Potential Targets	0°	5°	15°	30°	45°	60°
Flat Aluminum Sheet (Specular finish, Alzak)	347	7.4	.58	.50	.40	
Brass Tube (polished, 4" dia.)	8.2	3.2	.91	.35	~.25	~.21
*75 mm Shell, O.D. paint	.35	.31	.20	~.11	~.09	
*75 mm Shell (bright steel)	6.2	1.3	.37	~.11	~.08	
Flat black alkyd resin paint (on flat surface)	0.19					

* Type HEP-T165E11

Potential Terrains	Sensing Angle (off normal) 0°	5°	15°	30°	45°	60°
Pure white quartz (No. 16 graded ottowa sand)	2.1	2.1	2.0	1.9	1.6	1.3
White marsh concrete sand	1.62	1.62	1.60	1.49	1.32	1.08
No. 8-4 White marsh gravel	1.57	1.57	1.52	1.44	1.27	1.08
No. 4-3/8 " " "	1.70	1.70	1.68	1.57	1.40	1.24
No. 4-3/8 Iowa dolomitic limestone	1.09	1.10	1.12	1.10	1.12	1.13
common grass (cut)	.75	.71	.65	.58	.50	.47
dead brown leaves	~1.37	~1.37	~1.34	~1.1	~1.0	~0.8

In addition to those surfaces listed, reflectivity measurements will be made of snow and of mud.

At a sensing angle of about 30° and an altitude of about 3 feet, a negative-going pulse (not positive) is obtained when 75 mm O. D. shells are fired in daylight over a terrain background of a mixture of soil and grass.[1] Reference to the reflectivity data indicates that a negative signal is due to the greater reflectance of the terrain (obscuration by the shell). For increasing altitudes, the missile subtends a smaller amplitude. For night operation (sources on), the geometry is complicated by the fact that the flux incident on the target differs from that on the background. Laboratory measurements on birch-wood pellets have indicated a region of ambiguity; i.e., for sources on, as in night operation, there is an altitude at which the background reflection obscured by the pellet equals the energy reflected by the pellet. A similar investigation will be made for 75 mm rounds to determine the parameters for zero net return signal.

[1] For daytime operation, the system lights were turned off.

5. Sensing Resolution

Sensing accuracy or 'resolution' may be considered under the five categories of determining

a) The angle of incidence (angle ϕ in figure 1)

b) The displacement of the trajectory parallel to itself

c) Altitude

d) Velocity

e) Encounter time

Preliminary measurements have been made on b, c, d and e only.

Signal vs. Parallel Displacement

Figure 12 indicates the P. D. resolution of a screen sub-element for an arbitrarily selected set of conditions. These data were obtained with the large air gun using 4" diameter Styrofoam cylinders (simulated missiles) at normal incidence and at an altitude of 30". The line of flight is perpendicular to the line joining the detector and source (i.e., into the figure). For a fixed flight direction the sub-element was translated along the line joining the centers. It is evident from the figure that the sensing axis of the sub-element is nearly coincident with the detector axis. The signal is down ten-fold for a missile axis-detector axis displacement of about 3.7" at a 30" altitude. At greater altitudes a larger axis displacement would be required for equivalent signal degeneration. Figure 13 shows the overlap of the detection pattern of any 3 adjacent sub-elements in a screen. It is obvious that P. D. resolution may, if desired, be increased by narrowing the beam width, θ, and reducing the separation "c". The beam width may be narrowed by using either a longer focus paraboloid, a smaller detector area, or both. These factors have not been explored in the report period.

Altitude and Velocity

The 3 sub-element in-line sensing screen has been employed to determine the resolution of these parameters. From a typical oscillogram (e.g. figure 11B, oscillogram 1M) the pulse separation in time may be directly measured. This photo was made with the DOFL air gun using the arrangement shown in figure 4. The slant ranges and angles of incidence are shown in figure 14. The errors in altitude and velocity are within the experimental error (about 5%) of estimating pulse peaks on the photograph. Thus, in oscillogram 1M the 'true' velocity is 685 fps; the measured velocity is 670 fps; the 'true' slant range for beam b_2 is 37"; the measured range is about 40".[1] The displacement of the first two parallel beams was 12", measured along the direction of firing; the angular separation of the 2nd and 3rd beams was 15°. At the 30" slant range the separation of these 2 latter beams was 19.7". The true system error in measuring altitude and velocity is estimated to be less than 2% and is due to individual variations in reflectors, detectors, focussing, etc.

Encounter Time

The encounter time shall be defined as that time at which an acceptable target has been recognized in one or more elements of the outermost screen, thereby establishing a time base ($T = T_0$). It is evident that the subsequent passage through the two remaining screens will completely establish the trajectory

$$d = d(T)$$

where d = displacement in the horizontal plane of attack

[1] The second 'signal' in beam b_2 as seen in the photo should be ignored. It is due to the Styrofoam round striking the backstop, disintegrating, and rebounding into the last beam.

T = time

d_o = encounter 'point'

T_o = encounter time

Because of geometrical and physical considerations the encounter time will occur after the target ogive has reached the first detector axis. Figure 15 (oscillogram 6c) gives the encounter time delay and round position in time for the case of a 75 mm HEP round. The separation of beam 0 (1st detector axis) and a pulse 0 (peak of 1st pulse) is 250 μs. The experimental parameters are given in the figure. The two broken traces at the top were produced by passage of the round through two aluminum foil "make" circuits spaced 48" apart. The cross-hatched areas indicate the 1/2 power-point beam widths in the plane of encounter.

VIII. DOFL TEST AREA

Some preliminary data has been obtained on the sensing screen response at the DOFL Test Area using 75 mm shells in daylight operation (sources off.) Figure 11C shows two typical oscillograms (4F and 2F) for velocities of about 1540 fps and about 2500 fps respectively. Figure 15 is an analysis. It should be noted that the signals are negative (obscuration effect). The field arrangement is shown in figures 16, 17 and 18. In the foreground of figure 17 a simple optical trigger which initiates a single sweep on the cathode ray tube (not shown). Mounted below the sensing sub-screen are two aluminum foil 'make' circuits which locate the arriving round in relation to the three received signals and which serve to independently check missile velocity. These foils are located 48" apart and their output is visible on the oscillograms 6c and 2F as a pair of very steep spikes on the upper trace. The circular holes seen in the foils were produced by the actual firing. In the background is a mound of earth for stopping the missiles. All instrumentation is contained in the mobile laboratory

IX. SPECIAL CONSIDERATIONS

1. Velocity Discrimination

A successful system will ignore all potential targets with velocities less than about 200 fps. It will also be necessary to ignore all spurious signals due to the motion of the tank over irregular terrain, passing close to objects, cloud movement, personnel movement, etc. Such discrimination may be achieved by utilizing time gate techniques.

The first pulse or part of it (beam b_0, figure 19) initiates a finite time gate corresponding to a transit time of 200 fps for the target. Signal rejection occurs when the second pulse (beam b_1, figure 19) arrives too late.

2. Ignoring Small Arms Fire

'Small arms' refers to all missiles of lesser calibre than the smallest anti-tank round commonly used, i.e., less than about 37 mm.

Although small arms fire would produce weaker signals, it does not seem practicable to utilize signal amplitude as a basis for rejection since it would be difficult to distinguish between a small object close by and a larger object farther away unless more intelligence were built into the system.

It should, however, be possible to take advantage of the pure system geometry to achieve small arms rejection. Reference to figure 1 and figure 13 indicates that both the beam width, θ, and beam separation "c", could be chosen, that, for normal incidence at least, the number of adjacent detectors alerted in any screen would be well-defined function of altitude and and missile diameter. Thus for any particular altitude of attack, a minimum missile diameter could, in principle, be 'sensed'.

3. Effect Of Environment On Signal

With increasing temperature, the time constant, S/N, and dark resistance decrease (figure 20A) and the long wavelength cutoff shifts to somewhat shorter λ (see figure 20B). With increasing relative humidity the time constant increases rapidly (figure 20C). Increasing the ambient radiation level produces an effect similar to that of increasing the cell temperature. The

response of the bare cell is quite linear up to incident intensities of about 4300 μwatts/cm^2. This is a derived figure taken from data presented in figure 20D. For a 1 mm x 1 mm cell this represents 43 μwatts of energy.

4. Signal Ambiguity

Current work at the DOFL Test Area with 75 mm O. D. shells has indicated no ambiguity region in passing from daylight through twilight and into darkness. That is, negative signals have been recorded both day and night with signal level about 5-fold down at night. The sensing distances used at the DOFL Test Area are identical to those given in figure 14, with the exception that the "background level" of figure 14 is about 42" below the shell trajectory.

5. Reliability Of Cells

The cells used in the 3-sub-element test unit have shown no deterioration with age over the past seven months. They have been in use in both the DOFL air gun and the DOFL Test Area and have been exposed in the course of test work to an ambient temperature range of from about -5° C to +28°C and a relative humidity range from about 15% to about 90%.

ACKNOWLEDGEMENTS

The authors wish to thank Mr. W.S. Hinman, Jr., Technical Director of DOFL for suggesting an optical approach to the "Dash-Dot" problem. We are also grateful to Mr. E. Katzen for building circuitry and test equipment and making many valuable contributions in the course of this program. We also wish to acknowledge the co-operative spirit shown by Mr. Robert B. Burton of the DOFL Test Area.

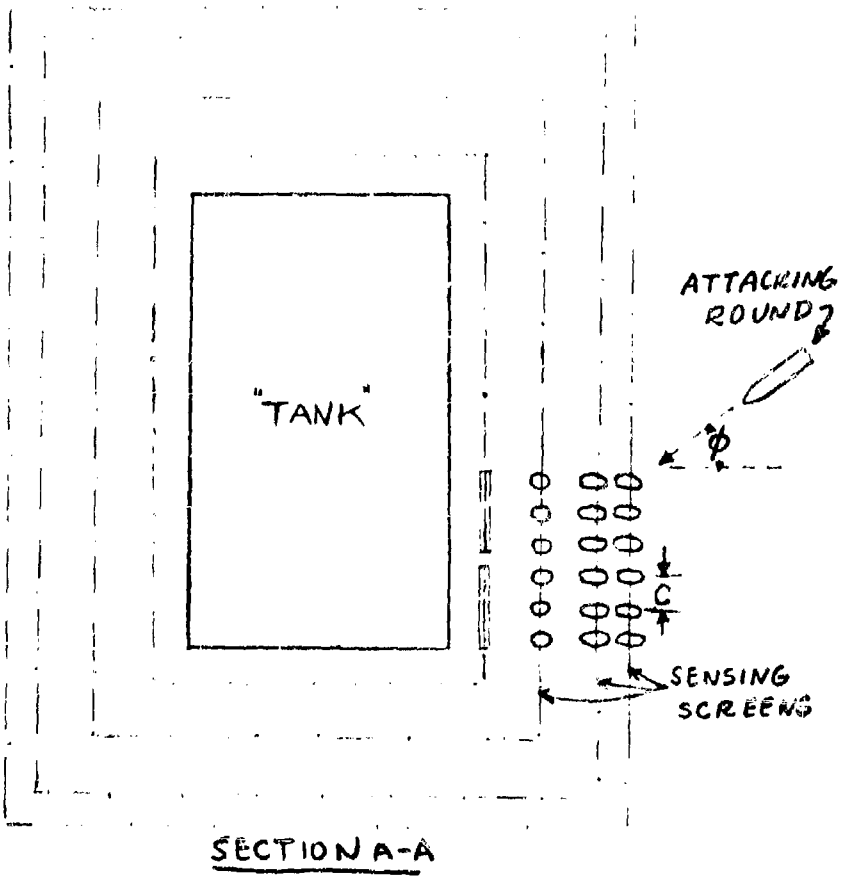

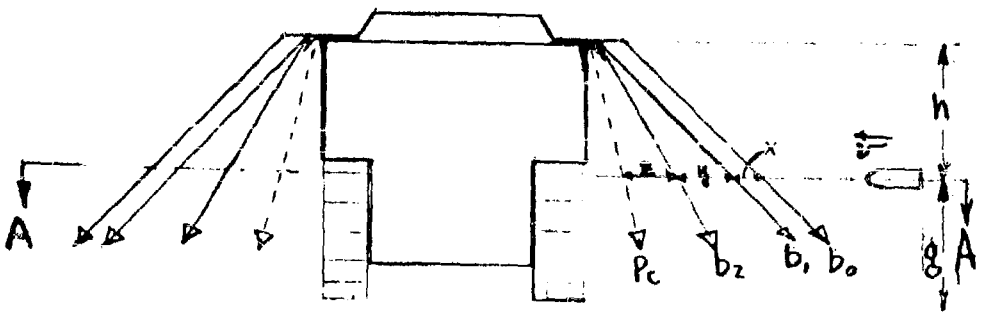

Figure 1. Outline of a Dash-Dot Geometry.

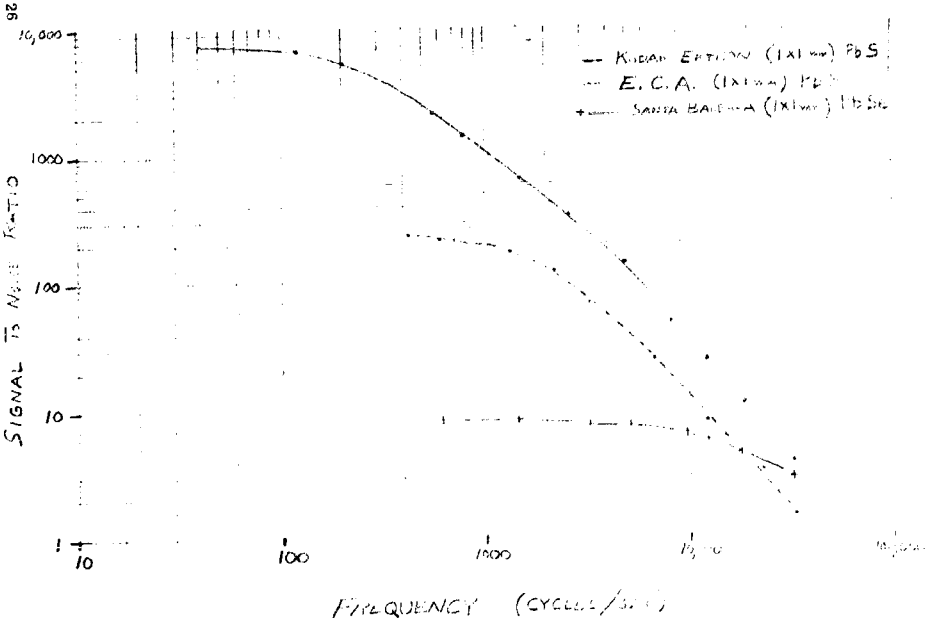

Figure 2. Signal-to-Noise Ratio vs. Frequency

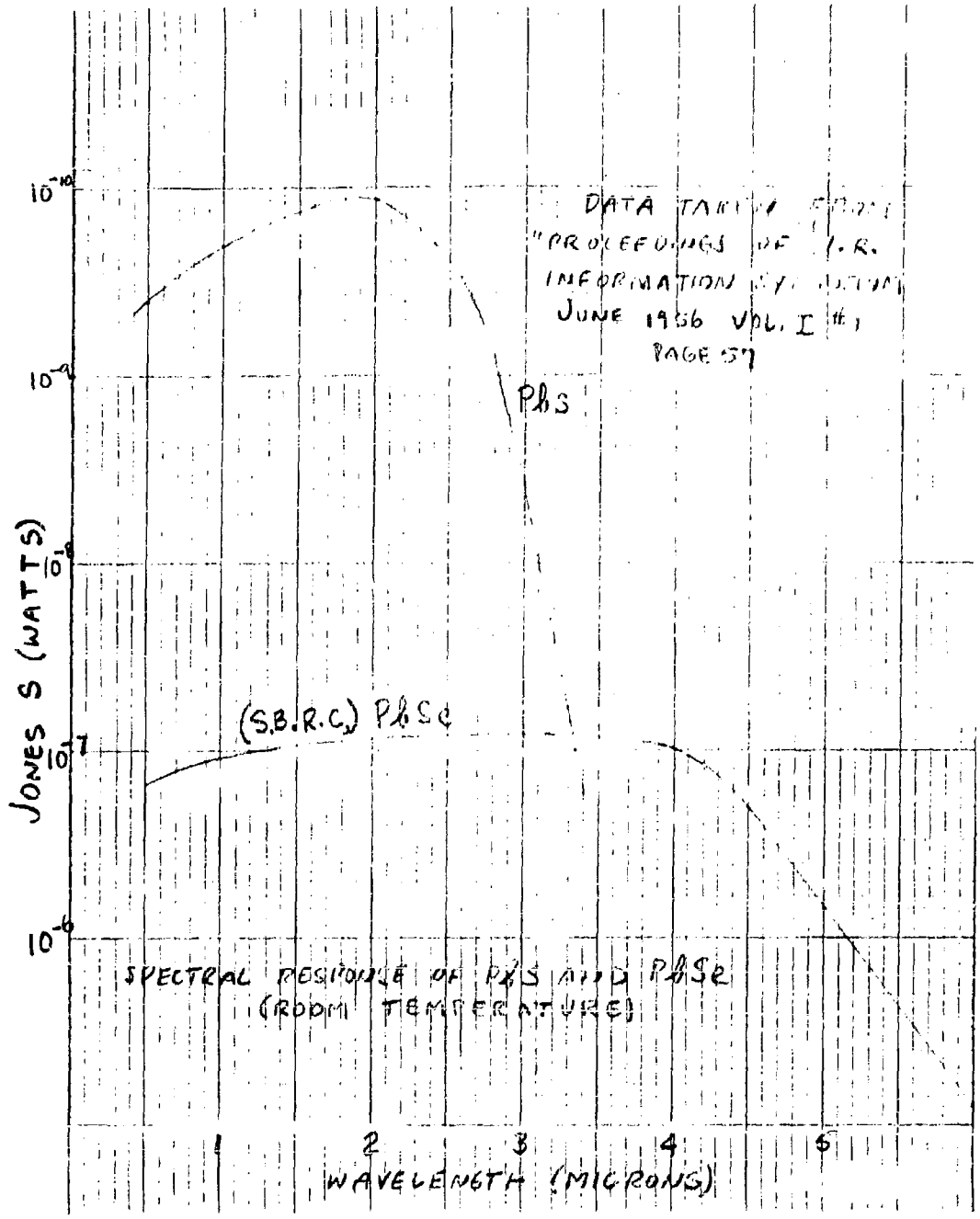

Figure 3. Spectral Response of PbS and PbSe(Room Temperature).

Figure 4. 3-Element Single Row Sub Screen.

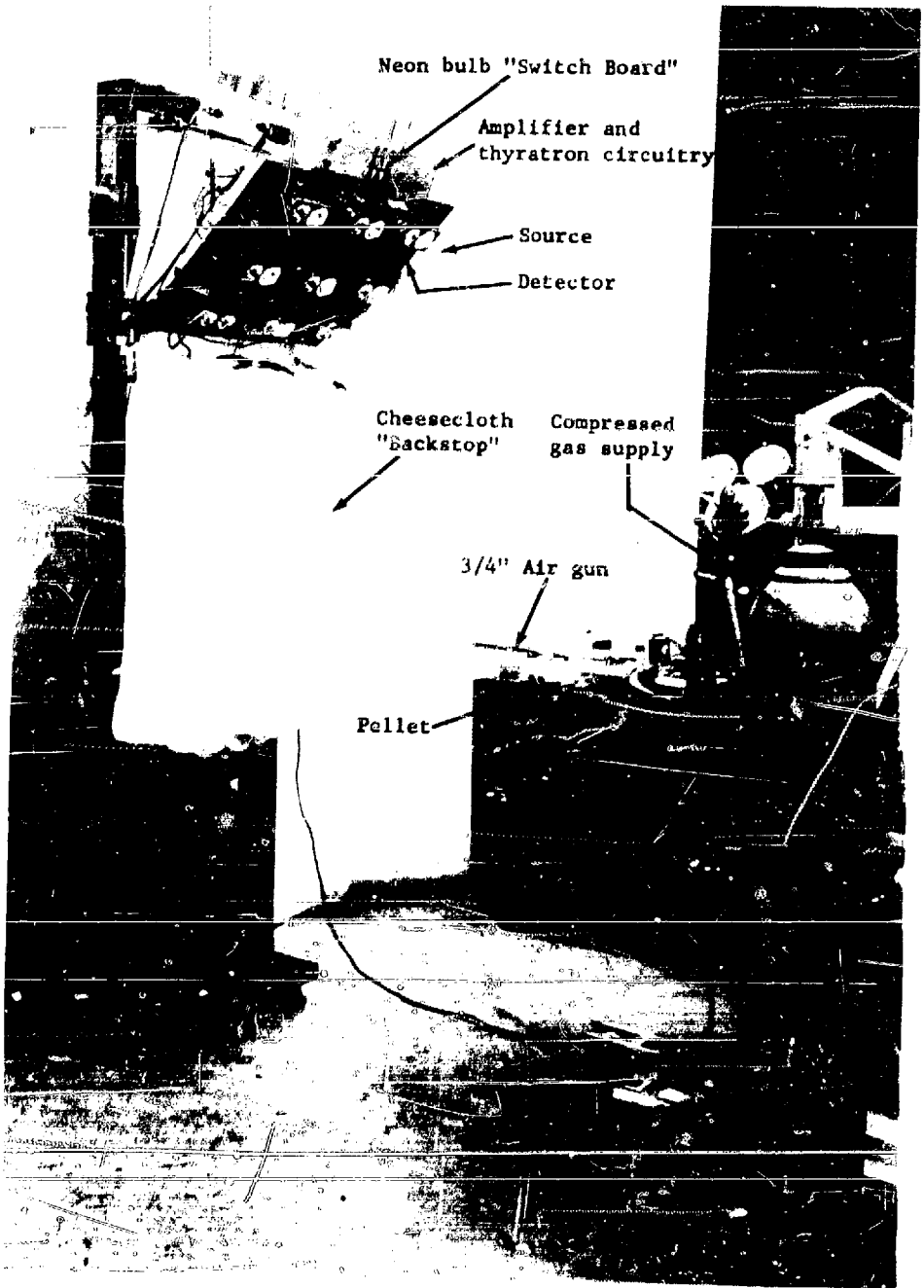

Figure 5. 9-Element Triple Row Sub-Screen.

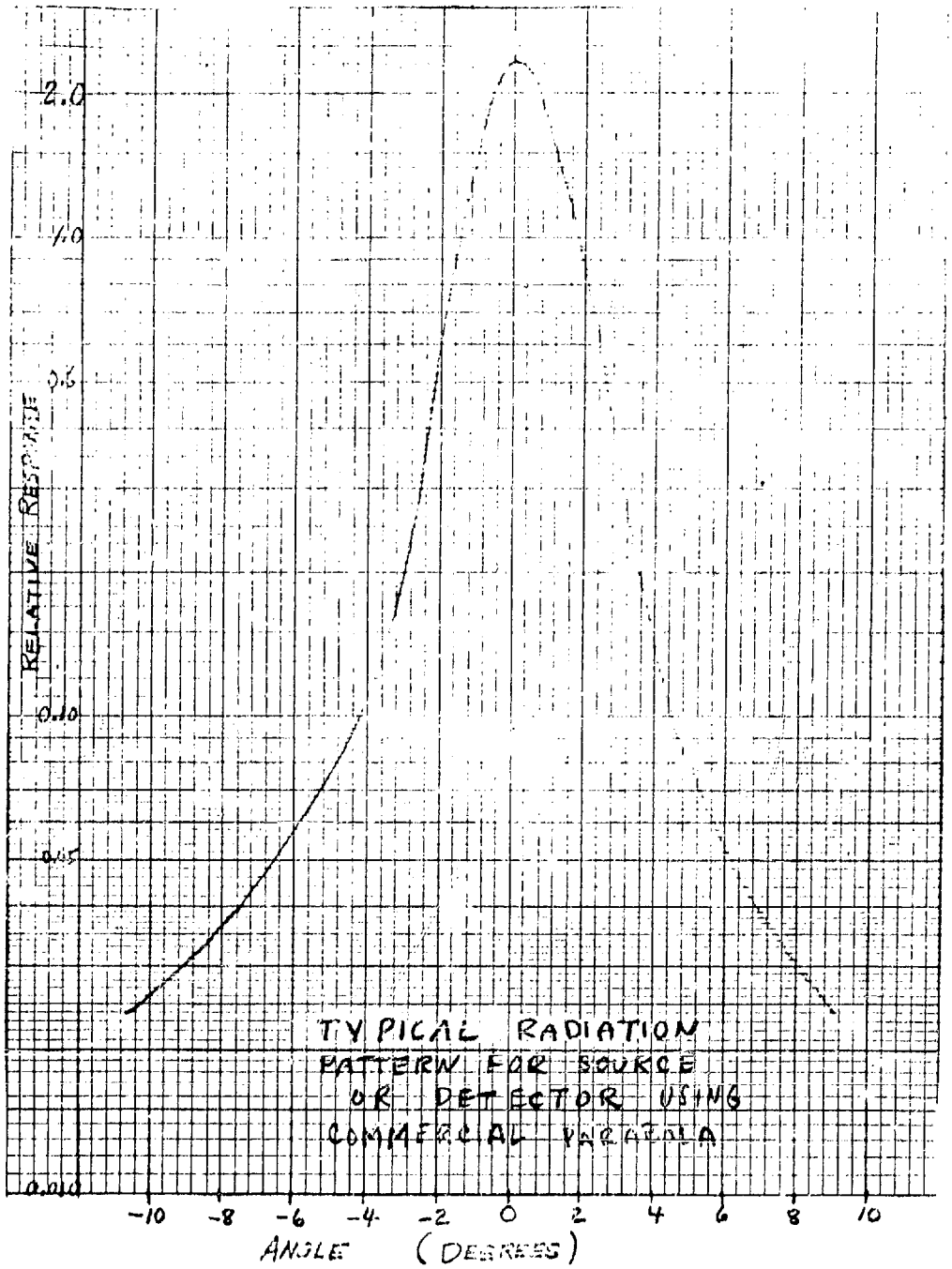

Figure 6. Typical Radiation Pattern for Source or Detector.

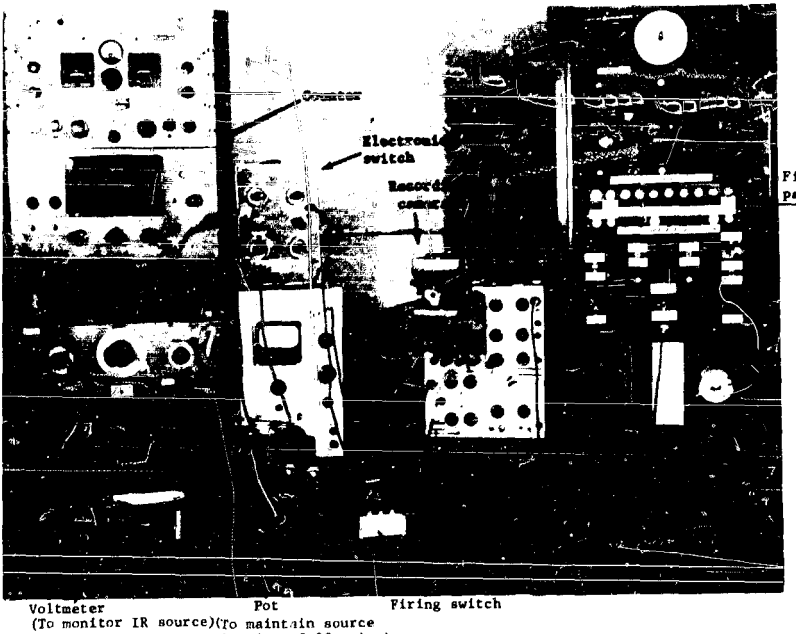

Figure 8. Instrumentation Adjacent to Air Gun Firing Room.

SECRET

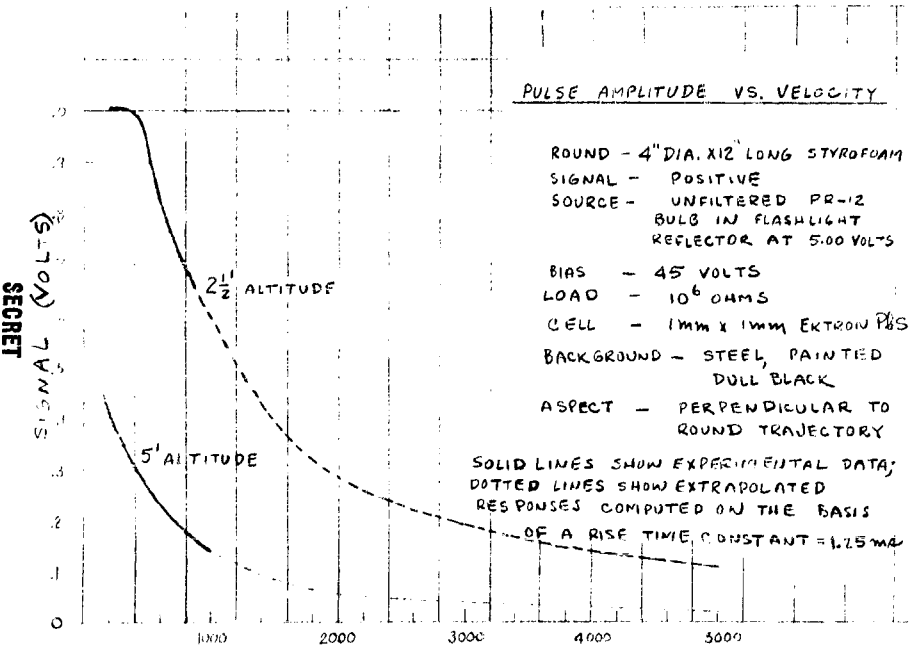

Figure 9. Pulse Amplitude vs. Round Velocity.

(A)

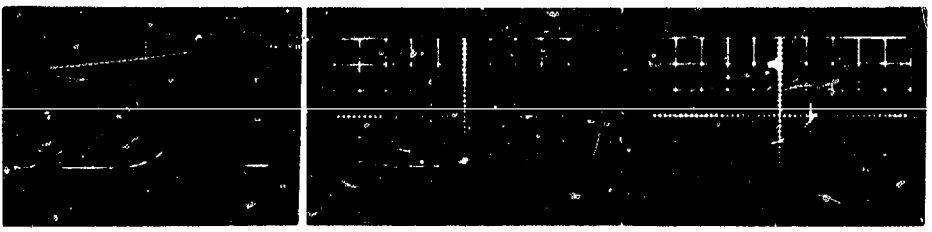

1	7	5
Sweep= 2 ms/cm Sensit= 0.2 v/cm	Sweep= 2 ms/cm Sensit= 0.2 v/cm	Sweep= 1 ms/cm Sensit= 0.2 v/cm

FIRING DIRECTION

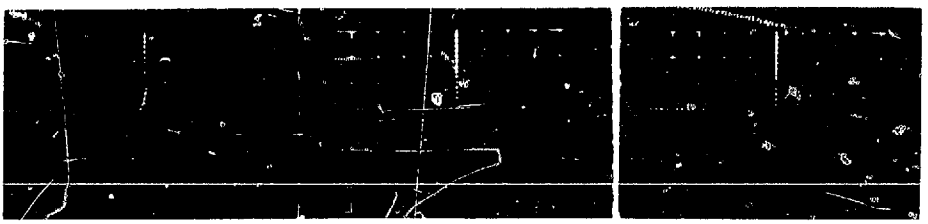

4	7	9
Sweep= 2 ms/cm Sensit= 0.1 v/cm	Sweep= 2 ms/cm Sensit= 0.05 v/cm	Sweep= 1 ms/cm Sensit= 0.05 v/cm

Figure 11A. Typical Pulse Oscillograms.

(B)

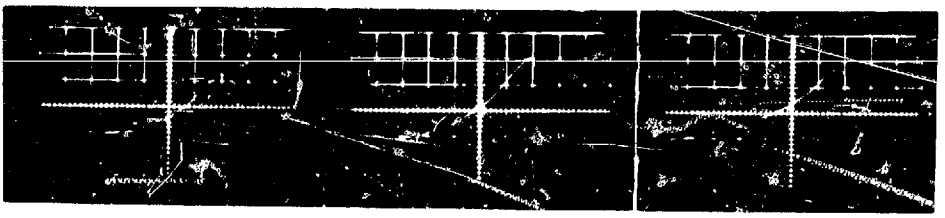

1D

Sweep= 1 ms/cm
Sensit= 0.2 v/cm

3D

Sweep= 1 ms/cm
Sensit= 0.1 v/cm

4D

Sweep= 1 ms/cm
Sensit= 0.05 v/cm

FIRING DIRECTION

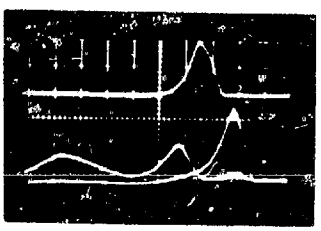

1M

Sweep= 2 ms/cm
Sensit= 0.5 v/cm

Figure 11B. Typical Pulse Oscillograms.

(C)

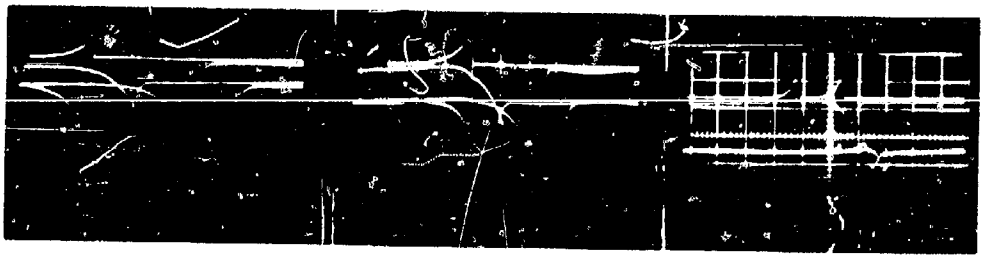

4F	2F	6C
Sweep= 0.5 ms/cm Sensit= 0.2 v/cm	Sweep= 0.5 ms/cm Sensit= 0.1 v/cm	Sweep= 1 ms/cm Sensit= 0.2 v/cm

FIRING DIRECTION

Figure 11C. Typical Pulse Oscillograms.

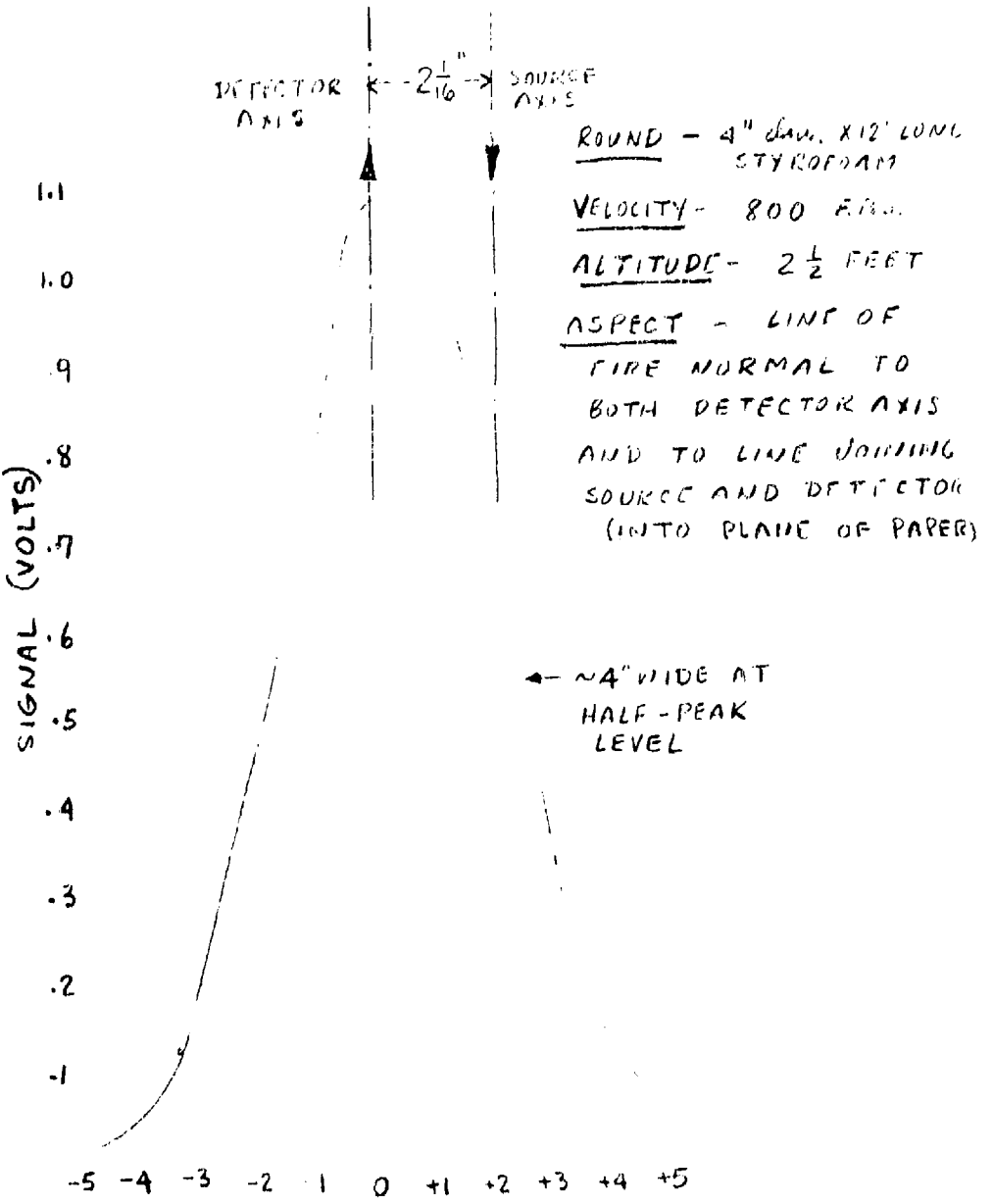

Figure 12: Signal vs. Parallel Displacement.

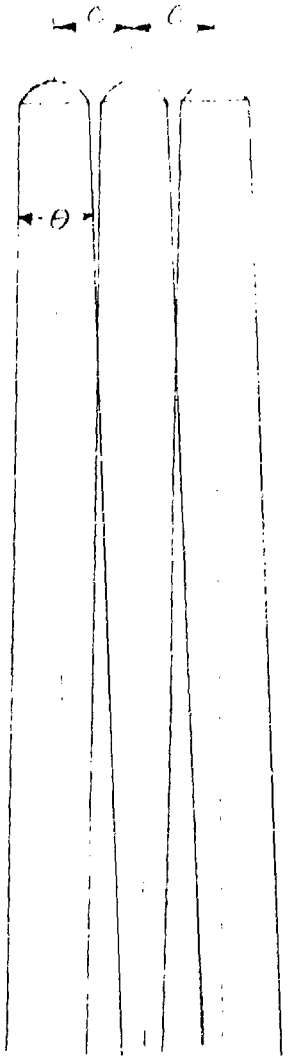

Figure 18. Overlap of Detection Patterns.

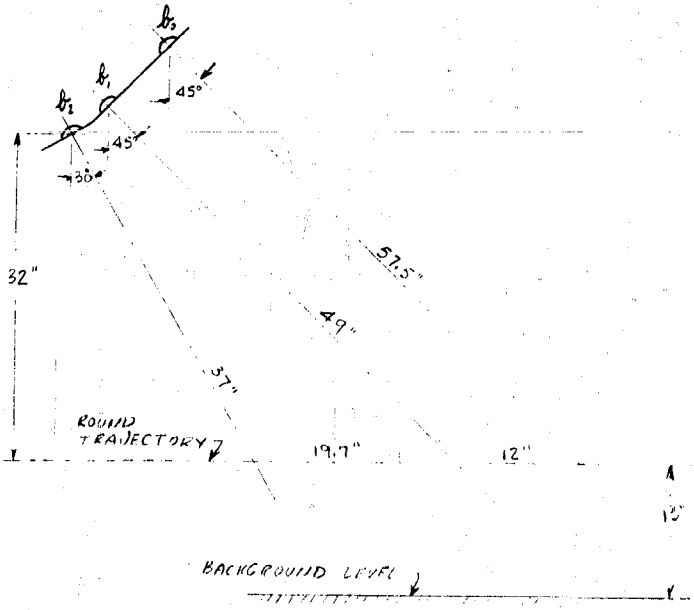

Figure 14. Typical Detecting Geometry.

SECRET

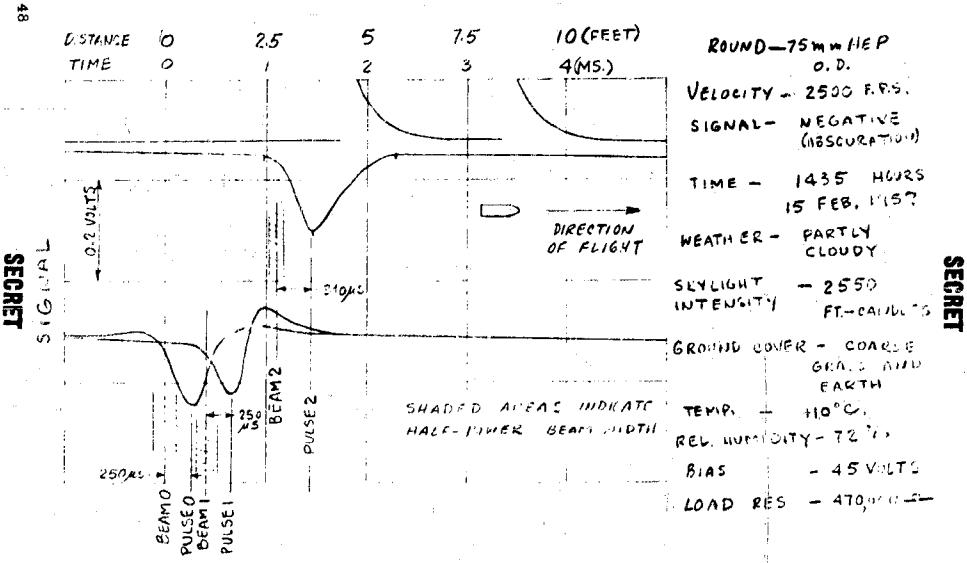

Figure 15. Typical Signal Pulses, 3-Element Sub-Screen.

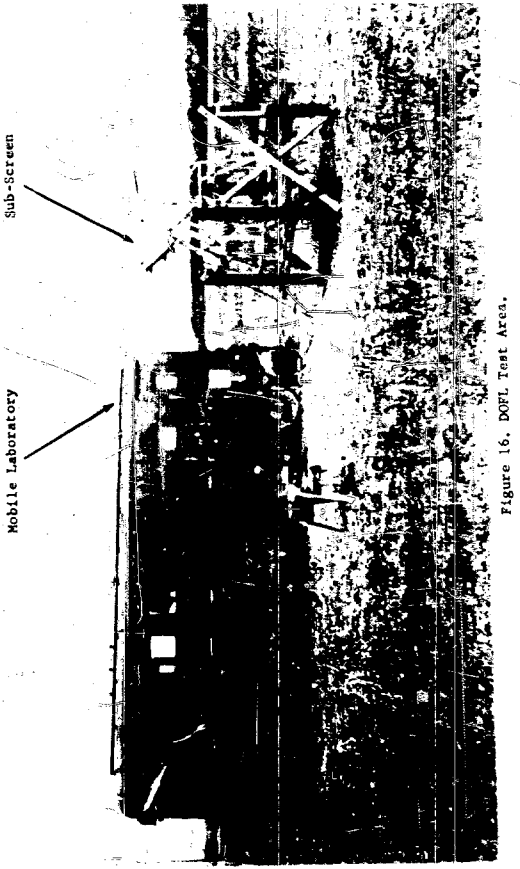

Figure 16. DOFL Test Area.

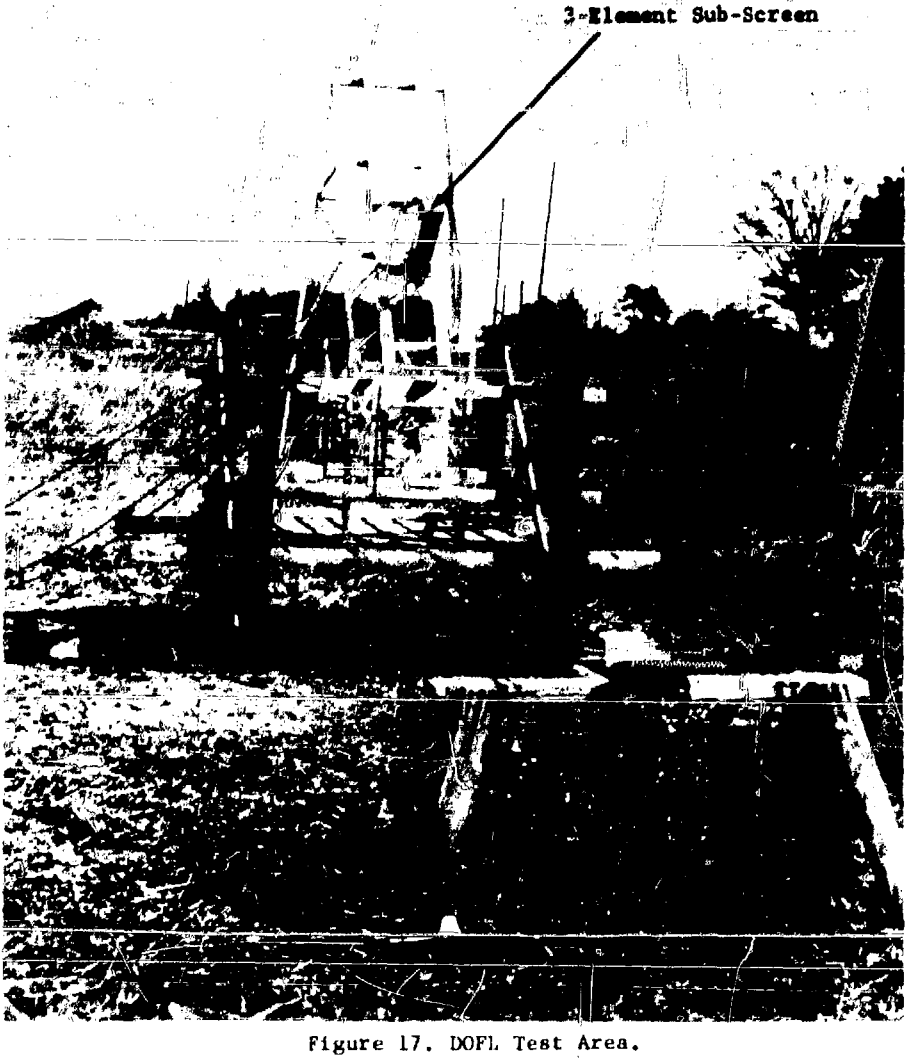

Figure 17. DOFL Test Area.

Figure 18. DOFL Test Area.

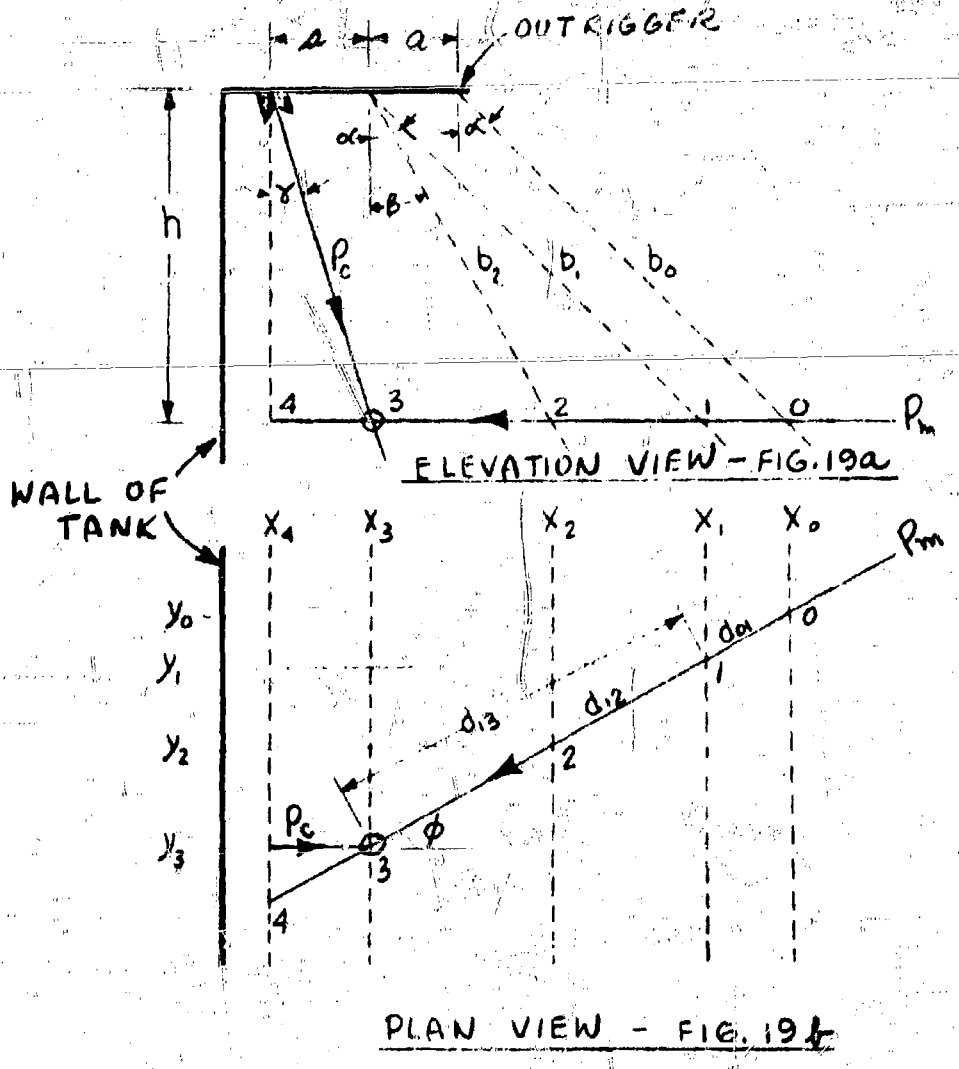

Figure 19. Diagram of Defending Screens.

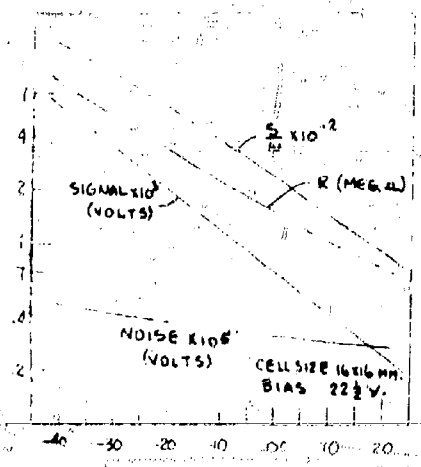

EFFECT OF TEMPERATURE ON RESISTANCE, SIGNAL, AND NOISE

20-A

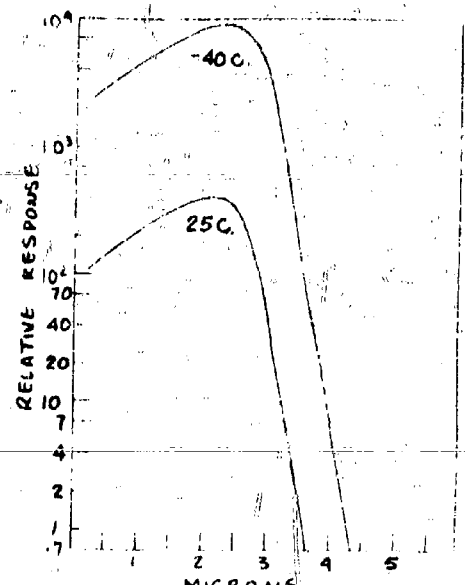

SPECTRAL RESPONSE

20-B

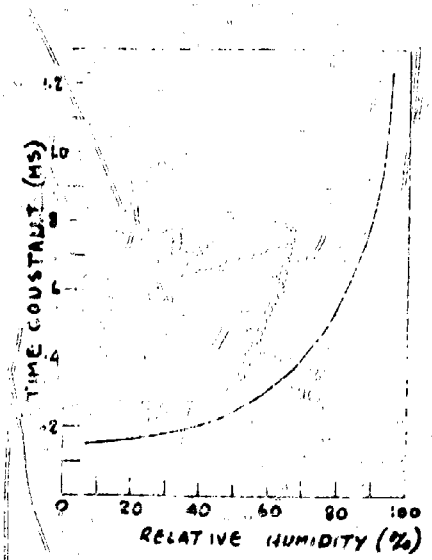

20-C

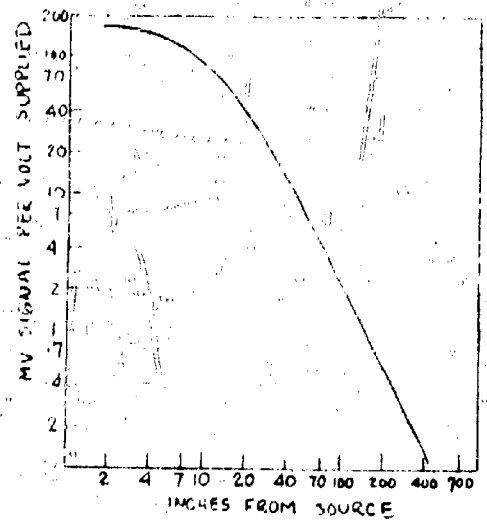

RESPONSE OF BARE PbS CELL TO A #1133 AUTO BULB (6V.-32CP)

20-D

Figure 20. Effects of Environment on Signal.

A, B, C, D reproduced from Kodak Pamphlet U-2 (Kodak Ektron Detector).

APPENDIX

Equations for Firing Time and Position of Defending Charge[1]

by

O. Cruzan, H.W. Kohler and H.W. Straub

The tank is surrounded by three optical screens consisting of sensing beams b_0, b_1, b_2 (figure 19) which are shown originating from an outrigger at the tank wall. Two of the screens are parallel, making an angle α with the vertical, and have a horizontal spacing "a". The third screen originates at the same place as the second screen, and makes an angle β with the vertical. The defending charges are arranged along a line parallel to the base of the three screens at a distance s from the intersection of the second and third and their trajectories make an angle γ with the vertical. The sensing beams b_0, b_1, b_2 and the trajectories p_c of the defending charges lie in planes parallel to that of figure 19a.

A projectile approaches from the right along a straight, horizontal trajectory P_m. Its velocity V_m, its horizontal angle ϕ of attack and its height "h" of attack are unknown. It traverses the beams b_0, b_1, b_2 at points 0, 1, 2 at times T_0, T_1, T_2. The times T_0, T_1, T_2 are measured, and the coordinates y_0, y_1, y_2 of the origins of the traversed beams are known[2]. Before the projectile reaches point 3, a defending charge located at coordinate y_3 is triggered at the right firing time T_f so that its fragments, which move at a velocity V_c, arrive at point 3 at the same time as the projectile.

The computer determines from the given parameters a, s, α, β, γ, V_c, and from the measured data y_0, y_1, y_2, T_0, T_1, T_2 the firing time T_f and the coordinate y_3 of the charge to be fired, and generates and transmits at the time T_f a triggering pulse to the charge positioned at y_3 so that the desired

---

1) For a more general presentation see, DOFL TR- 433, "Theoretical Analysis of a Dash-Dot Sensing System" by O.R. Cruzan.

2) Note that the coordinates x_0, x_1, x_2 are not known, being functions of the unknown height "h" of attack.

tor).

collision occurs.

The equations for which the computer has to be designed will now be derived.

Equation for Firing Time T_f

In order to obtain a collision at point 3, there must be

$$T_f + T_c = T_3, \tag{1}$$

where T_f is the firing time, T_c the transit time of the charge fragments to point 3, and T_3 the time of arrival of the projectile at point 3.

For T_c one gets from figure 19a

$$T_c = \frac{h}{V_c \cdot \cos \gamma} . \tag{2}$$

where h is the height of attack, and V_c the velocity of the defending charge fragments. Substituting in (1)

$$T_f = T_3 - \frac{h}{V_c \cdot \cos \gamma} \tag{3}$$

T_3 and h are not known and have to be determined from known parameters and data.

For h, one uses the equation

$$\frac{T_1 - T_0}{T_2 - T_1} = \frac{d_{01}/V_m}{d_{12}/V_m} = \frac{d_{01}}{d_{12}} \tag{4}$$

where d_{01} and d_{12} are the distances of points 0 to 1 and 1 to 2, respectively, on the projectile trajectory, and V_m is the projectile velocity.

Elementary geometry shows that

$$\frac{d_{01}}{d_{12}} = \frac{x_0 - x_1}{x_1 - x_2} \quad \text{and} \tag{5}$$

$$x_0 - x_1 = a \tag{6}$$

For $x_1 - x_2$ one gets from trigonometry

$$x_1 - x_2 = (h \cdot \tan \alpha + a) - (h \cdot \tan \beta + a)$$

$$= h(\tan \alpha - \tan \beta) \tag{7}$$

therefore

$$\frac{d_{01}}{d_{12}} = \frac{a}{h \cdot (\tan \alpha - \tan \beta)} \tag{8}$$

Substituting (8) in (4) and rearranging:

$$h = \frac{a}{\tan \alpha - \tan \beta} \cdot \frac{T_2 - T_1}{T_1 - T_0} \tag{9}$$

For T_3 one may use an equation like

$$\frac{T_3 - T_1}{T_1 - T_0} = \frac{d_{13}/V_m}{d_{01}/V_m} = \frac{d_{13}}{d_{01}} \tag{10}$$

where d_{13} is the distance between points 1 and 3 on the projectile trajectory.

Again from geometry, and remembering that $x_0 - x_1 = a$, one gets

$$\frac{d_{13}}{d_{01}} = \frac{x_1 - x_3}{a} \tag{11}$$

Trigonometry gives for $x_1 - x_3$

$$x_1 - x_3 = h_1 \tan\alpha + s - h_3 \tan\gamma$$

$$= h(\tan\alpha - \tan\gamma) + s \tag{12}$$

Substituting (12) in (11), (11) in (10), and rearranging:

$$T_3 = T_1 + \frac{h(\tan\alpha - \tan\gamma) + s}{a}(T_1 - T_0) \tag{13}$$

If one now introduces in (3) the value of h from (9) and that of T_3 from (13), one gets finally

$$T_f = T_1 + \frac{\tan\beta - \tan\gamma}{\tan\alpha - \tan\beta}(T_2 - T_1) - \frac{s}{a}(T_1 - T_0)$$

$$- \frac{a}{V_c \cos\gamma (\tan\alpha - \tan\beta)} \frac{T_2 - T_1}{T_1 - T_0} \tag{14}$$

Equation for Coordinate y_3 of Charge to be Fired

For the determination of y_3 one may use an equation like

$$\frac{y_3 - y_1}{y_1 - y_0} = \frac{x_1 - x_3}{x_0 - x_1} \tag{15}$$

which follows from geometry.

Substituting $x_1 - x_3$ from (12), and again remembering that $x_0 - x_1 = a$, one gets

$$\frac{y_3 - y_1}{y_1 - y_0} = \frac{h(\tan\alpha - \tan\gamma) + s}{a} \tag{16}$$

Introducing in (16) the value of h from (9) and rearranging finally yields

$$y_3 = y_1 + \frac{\tan\alpha - \tan\gamma}{\tan\alpha - \tan\beta}\frac{T_2 - T_1}{T_1 - T_0}(y_1 - y_0) + \frac{s}{a}(y_1 - y_0) \tag{17}$$

From equations (14) and (17), the position of the charge to be fired and its firing time are determined for any velocity of the oncoming projectile and for any height and angle of attack.

If the projectile trajectory cannot be approximated by a straight, horizontal line, an arrangement of more than three screens must be used.

Compilation of Equations for T_f and y_3

If in equations (10) and (15) combinations of T's and d's, y's amd x's other than those used had been chosen, equations for T_f and y_3 of different structures but giving the same ultimate values would have resulted. The following equations are obtained by changing the combinations. For the matter of simplicity, the abbreviations

$$Q = \frac{\tan\alpha - \tan\gamma}{\tan\alpha - \tan\beta} \tag{18}$$

and

$$P = (\tan\alpha - \tan\beta)\cos\gamma \tag{19}$$

are used.

$$T_f = T_0 + \left(\frac{s}{a} + 1\right)(T_1 - T_0) + Q(T_2 - T_1) - \frac{a}{V_c \cdot P}\,\frac{T_2 - T_1}{T_1 - T_0} \qquad (14a)$$

$$T_f = T_1 + \frac{s}{a}(T_1 - T_0) + Q(T_2 - T_1) - \frac{a}{V_c \cdot P}\,\frac{T_2 - T_1}{T_1 - T_0} \qquad (14b)$$

$$T_f = T_2 + \frac{s}{a}(T_1 - T_0) + (Q - 1)(T_2 - T_1) + \frac{a}{V_c \cdot P}\,\frac{T_2 - T_1}{T_1 - T_0} \qquad (14c)$$

$$y_3 = y_0 + Q\,\frac{T_2 - T_1}{T_2 - T_0}(y_2 - y_0) + \left(\frac{s}{a} + 1\right)\frac{T_1 - T_0}{T_2 - T_0}(y_2 - y_0) \qquad (17a)$$

$$y_3 = y_0 + Q\,\frac{T_2 - T_1}{T_1 - T_0}(y_1 - y_0) + \left(\frac{s}{a} + 1\right)(y_1 - y_0) \qquad (17b)$$

$$y_3 = y_0 + Q(y_2 - y_1) + \left(\frac{s}{a} + 1\right)\frac{T_1 - T_0}{T_2 - T_1}(y_2 - y_1) \qquad (17c)$$

$$y_3 = y_1 + Q\,\frac{T_2 - T_1}{T_2 - T_0}(y_2 - y_0) + \frac{s}{a}\,\frac{T_1 - T_0}{T_2 - T_0}(y_2 - y_0) \qquad (17d)$$

$$y_3 = y_1 + Q\,\frac{T_2 - T_1}{T_1 - T_0}(y_1 - y_0) + \frac{s}{a}(y_1 - y_0) \qquad (17e)$$

$$y_3 = y_1 + Q(y_2 - y_1) + \frac{s}{a}\,\frac{T_1 - T_0}{T_2 - T_1}(y_2 - y_1) \qquad (17f)$$

$$y_3 = y_2 + (Q - 1)\frac{T_2 - T_1}{T_2 - T_0}(y_2 - y_0) + \frac{s}{a}\frac{T_1 - T_0}{T_2 - T_0}(y_2 - y_0) \qquad (17g)$$

$$y_3 = y_2 + (Q - 1)\frac{T_2 - T_1}{T_1 - T_0}(y_1 - y_0) + \frac{s}{a}(y_1 - y_0) \qquad (17h)$$

$$y_3 = y_2 + (Q-1)\ (y_2 - y_1) + \frac{s}{a}\frac{T_1 - T_0}{T_2 - T_1}(y_2 - y_1) \qquad (17i)$$

From each of the above sets of equations (14 a to c) and (17 a to i) one equation has to be selected that promises a minimum of difficulties in designing the computer.

NOTIFICATION OF MISSING PAGES

INSTRUCTIONS: THIS FORM IS INSERTED INTO ASTIA CATALOGED DOCUMENTS TO DENOTE MISSING PAGES.

AD No. 307953
ASTIA FILE COPY

CLASSIFICATION (CHECK ONE)		
UNCLASSIFIED	CONFIDENTIAL	SECRET ✓

THE PAGES, FIGURES, CHARTS, PHOTOGRAPHS, ETC., MISSING FROM THIS DOCUMENT ARE:

MISSING PAGES ARE BLANK

DO NOT REMOVE